

Resistive switching in Si₂Te₃ nanowires

Keyue Wu, 1,2 Jiyang Chen,2 Xiao Shen,2 and Jingbiao Cui^{2,a}

¹College of Electrical and Photoelectronic Engineering, West Anhui University, Lu'an 237012, Anhui, People's Republic of China

²Department of Physics and Materials Science, The University of Memphis, Memphis, Tennessee 38152, USA

(Received 21 September 2018; accepted 24 November 2018; published online 7 December 2018)

As a silicon-based chalcogenide, semiconducting Si₂Te₃ has recently attracted attention as an emerging layered 2D material. Here, single-crystalline Si₂Te₃ nanowires (NWs) are synthesized by chemical vapor deposition (CVD). The Si₂Te₃ NWs grow along the [0001] direction, which is perpendicular to the 2D layers. The NWs exhibit a unique reversible resistance switching behavior driven by an applied electrical potential, which leads to switching of the NWs from a high-resistance state to a low-resistance state. This switched state is stable unless the opposite potential is applied to switch the resistance back. It is also noted that the polarity of the initially applied potential along the NWs defines the switch on and off directions, which become permanent once set. In combination with theoretical calculations, the resistance switching is explained by an internal structural change resulting from the applied potential. This novel resistance switching property for the silicon-based 2D materials is not only interesting for fundamental exploration but also holds promise for applications in memory devices. © 2018 Author(s). All article content, except where otherwise noted, is licensed under a Creative Commons Attribution (CC BY) license (http://creativecommons.org/licenses/by/4.0/). https://doi.org/10.1063/1.5060675

Si₂Te₃ is considered as a p-type semiconductor with a band gap in the visible region.¹ It has a unique crystal structure where Si atoms form dumb-bells sandwiched between the Te layers, i.e., Si-Si dimers exist in the sites between the hexagonally close-packed Te atoms.² Covalent bonds are formed between the Te and Si within each layer, while weak van der Waals bonding exists between the layers to form a layered crystal structure. A recent study showed that rotation of the Si dimer, with four possible orientations within the Si₂Te₃ layer, gives rise to a unique structural variability that could have potential new applications in electronic and optoelectronics devices.³ Recently, single-crystal Si₂Te₃, Ge-doped Si₂Te₃ nanoplates and Si₂Te₃ nanowires were synthesized by CVD method and their optical properties were studied.⁴⁻⁷ The achievement of doping Si₂Te₃ opens the door for tuning its electric properties for device applications.⁷ However, the electrical properties of Si₂Te₃ nanostructures have not been reported so far.

In this study, we investigated the structure and electrical properties of Si₂Te₃ nanowires. It was found that the nanowires grow along the c-axis, i.e., along the [0001] direction, with stacking of layered nanosheets via the van der Waals force forming single crystalline one-dimensional (1D) structures. The 1D NWs composed of 2D Si₂Te₃ material exhibit a unique resistance switching behavior under an applied potential. A stable low-resistance state (LRS) is defined by the initial voltage applied to a fresh NW. One can switch the LRS to the high-resistance state (HRS) by changing the polarity of the applied potential. Theoretical calculations suggest that electrically induced structural change plays an important role in the resistance switching property. This study indicates that the resistance switching behavior of the unique silicon-based Si₂Te₃ NWs is of great interest for both fundamental understanding and practical applications in memory devices.

The Si₂Te₃ NWs were synthesized by using CVD method as reported in our previous report.⁶ In brief, the NWs were grown on Au-coated Si or FTO substrates in a quartz tube at 650 °C by using



^aEmail address: jcui@memphis.edu

silicon and tellurium as sources materials. The Si_2Te_3 NWs grown on the edge of the FTO glass were used for electrical study by contacting the NWs with a liquid gallium electrode, while the conducting FTO on which the NWs grow was used as another electrode. A micromanipulator is used to move the gallium electrode and approach the NWs to make electrical contact while the electrical current is monitored. Note that the liquid gallium is used as an electrode to avoid mechanical damage to the NWs once physical contact is established.

Electronic properties of Si_2Te_3 were investigated by first-principles calculations based on density functional theory. ^{8,9} We use the PBE exchange-correlation functional, ¹⁰ plane-wave basis, and PAW potentials ¹¹ implemented in the VASP code. ¹² We use an energy of 245.3 eV for the plane-wave cutoff. For structural relaxation, a $4\times4\times2$ Monkhorst-Pack ¹³ k-point mesh is used for Brillouin zone sampling. For calculation of the electronic density of states, a Gamma-centered $9\times9\times5$ k-point mesh is used for Brillouin zone sampling.

The morphology and crystal structure of the Si_2Te_3 NWs were studied by scanning electron microscopy (SEM) and transmission electron microscopy (TEM), as shown in Figs. 1(a) and 1(b). One can see that the NWs show diameters ranging from tens to hundreds of nanometers and lengths of up to 60 μ m. Each NW has a very uniform diameter over the whole length scale and is mostly straight with Au at the tip of the nanowires.

Fig. 1(b) shows a typical TEM image obtained for a thin NW with a diameter of 40 nm. The HRTEM image in the inset of Fig. 1(b) clearly shows the fringes of the Si₂Te₃ NW, which indicates that the NW is composed of stacked layers packing along the [0001] direction via a weak van der Waals interaction. The periodicity for the alternating fringes along the NW growth direction is 0.65 nm, corresponding to the distance between the (0002) planes for hexagonal Si₂Te₃.² The SAED (selected area electron diffraction) pattern shown in the inset of Fig. 1(b) also confirms that the growth direction of the NWs is along [0001]. Energy-dispersive X-ray spectroscopy (EDX) was measured to determine the NW composition, which shows an elemental ratio of 2:3 for Si and Te in the NWs. The elemental composition was also confirmed by X-ray photoemission spectroscopy.

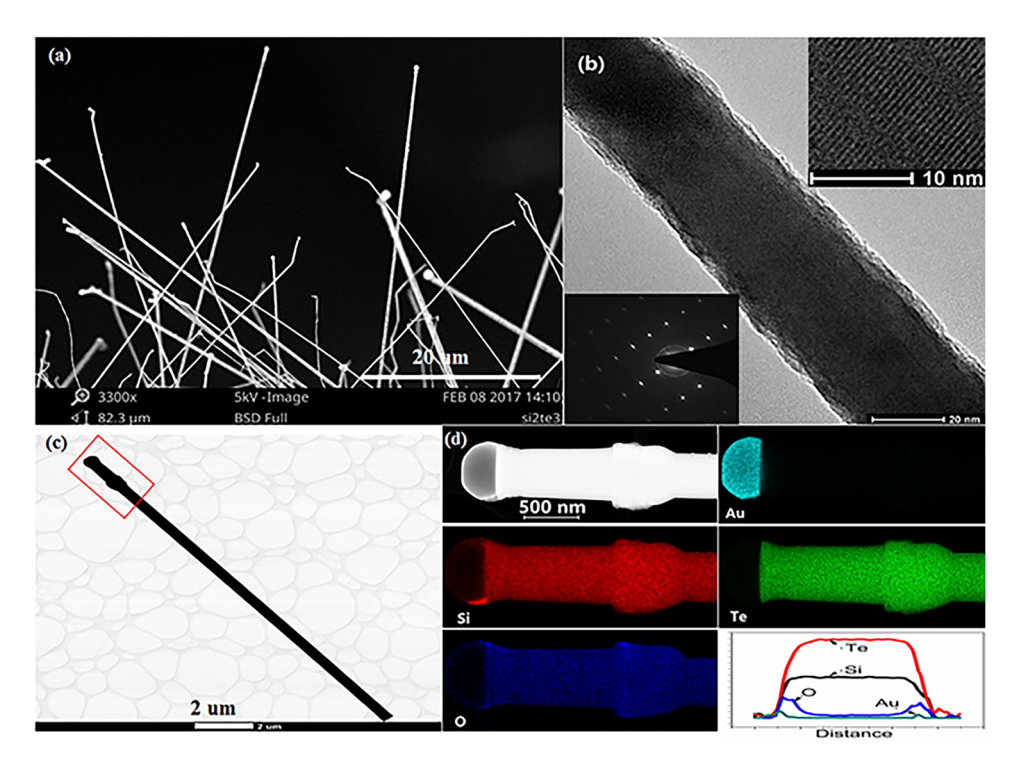


FIG. 1. SEM image for the Si_2Te_3 NWs (a), TEM image for a Si_2Te_3 NW (b), the insets in (b) show high-resolution TEM and SAED images for the NW, bright-field image of individual NW (c), and EDX elemental mapping for Au, Si, Te, O, and the cross-sectional line scan for each element (d).

Fig. 1(d) shows the TEM image, bright-field scanning transmission electron microscopy (STEM) image, and spatial distribution for the Si, Te, O and Au elements in a Si_2Te_3 NW. Au was found only at the tip of the nanowire. Both Si and Te are uniformly distributed across the nanowire. The EDX elemental line scans across the NW, as shown in Fig. 1(d), do not reveal a variation for the Si and Te elemental distribution within the nanowire. It is also noted that the O element exists on the surface of the nanowire. This is because the Si_2Te_3 has pronounced hygroscopic properties and its surface can easily react with water vapor when exposed to air. 14

The setup for electrical contact is plotted in the inset of Figure 2(a). As shown in Fig. 2(a), the current change with time measured under a constant voltage of 0.1 V for an NW moving towards the Ga electrode. The initial current is zero because there is no contact between the NWs and Ga electrode. As the Ga electrode approaches the Si₂Te₃ NWs, the current jumps from 0 to approximately 0.9 nA at 103 seconds, indicating that a nanowire is contacted with the Ga electrode. If one continues to move the Ga electrode toward the NW sample, the current stays constant until a second current jump from 0.9 to 1.8 nA is observed at approximately 107 seconds due to additional NW contact with the Ga electrode. Further moving of the Ga electrode closer to the NW sample leads to the observation of a large jump in the current of up to 7 nA, which may be caused by a large wire or a group of NWs contacting with the Ga electrode. As the stage with the Ga electrode moved away from the NWs, the current suddenly drops to 0.9 nA and further to zero. This experimental approach confirms that it is possible to make electrical contact with the fragile NWs using a liquid electrode and measure the current-voltage (I-V) curve for a single Si₂Te₃ NW. Once contact with the NWs by the Ga electrode is established, an I-V curve can be measured, as shown in Figure 2(b). A nonlinear characteristic is observed, which shows that the as-prepared Si₂Te₃ NW is a semiconductor. In the low voltage range between -1 and 1 V, the I-V curve is repeatable when sweeping the voltage back and forth. Note that the current for the individual NWs may vary due to their different diameters.

As shown in Fig. 3(a), resistance switching is observed in a freshly prepared Si₂Te₃ NW as the voltage was increased from 0 V, with a current jump at approximately 0.9 V. This sudden current

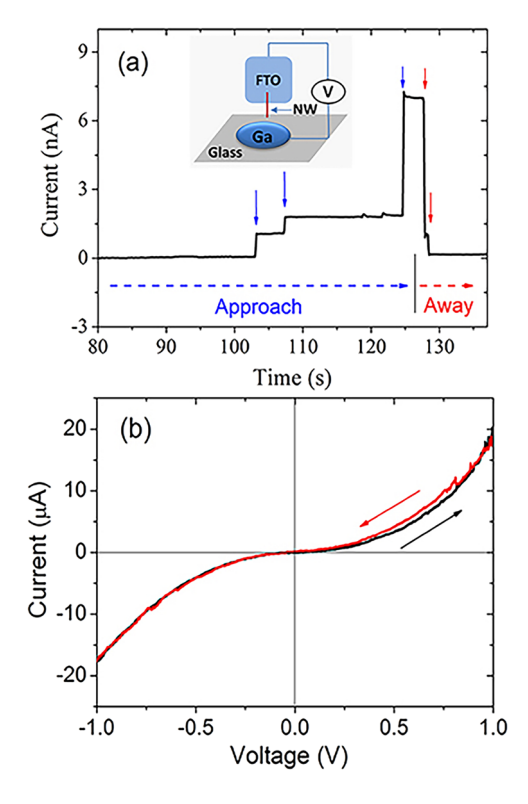


FIG. 2. (a) Variation in the current for Si2Te3 NWs under an applied voltage of 0.1 V as a gallium electrode is moved toward and away from the NWs; The inset of (a) is the setup for electrical measurement. (b) I-V curve measured between -1 and +1 V.

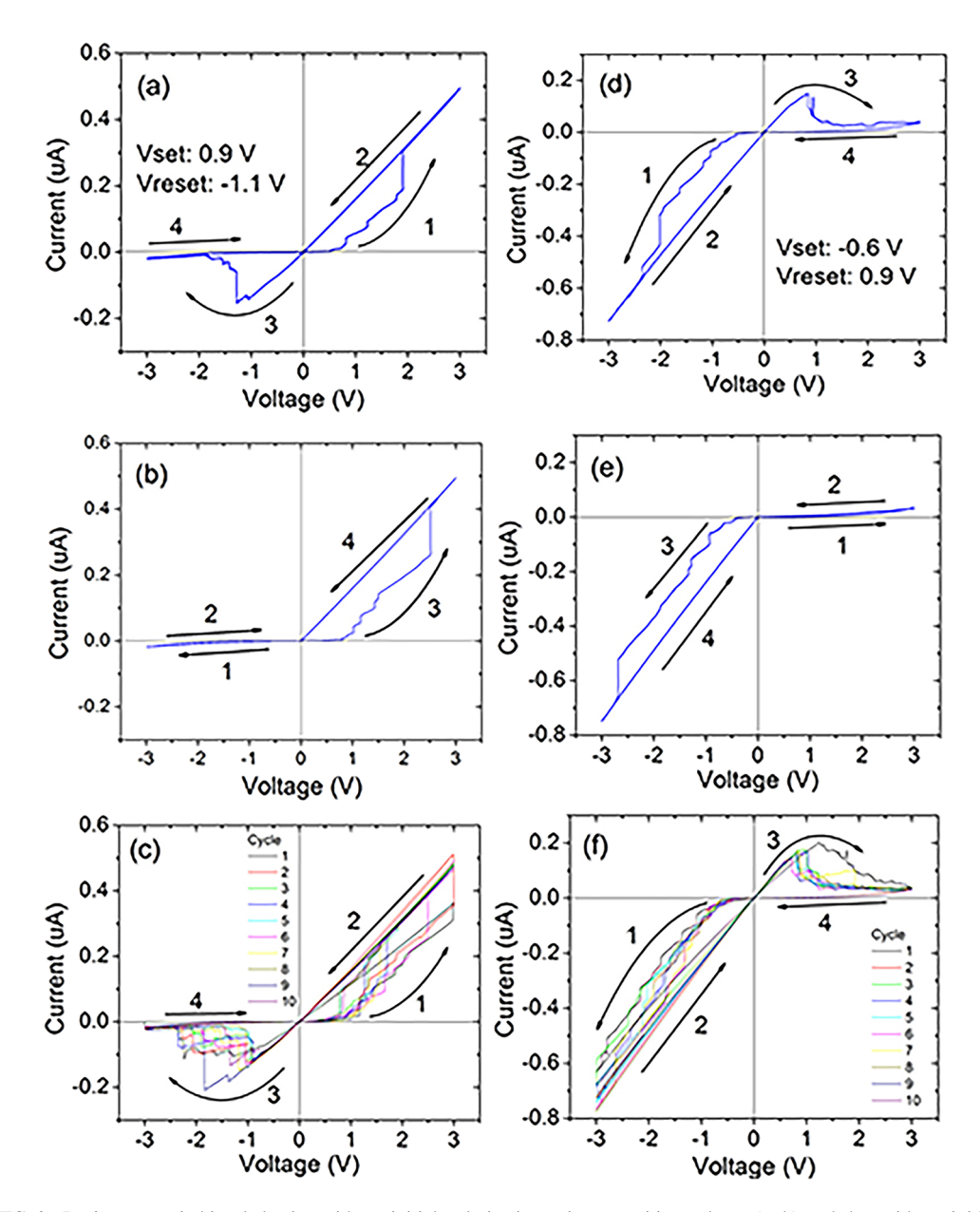


FIG. 3. Resistance switching behavior with an initial polarization using a positive voltage (a, b) and that with an initial polarization using a negative voltage (d, e). The positive voltage refers to the potential on FTO electrode. The voltage sweep sequences are indicated in the figures by arrows labelled 1, 2, 3, and 4. Repeated resistance switching under multiple scans (cycles) for positive (c) and negative polarized NWs (f).

jump from low to high corresponds to a sudden drop in resistance at the applied voltage. This process is referred to as SET for switching from LRS to HRS. If one continues to increase the voltage, a few current jumps occur at different voltages. When the voltage sweeps back from +3.0 to -3.0 V, the LRS is initially preserved until a negative voltage of -1.1 V is applied. This resistance switching from LRS to HRS is referred to as a RESET process. Further scanning of the voltage from -3.0 to 0 V does not change the resistance of the NW, which is actually the original resistance before the SET process. If an opposite voltage scan sequence is used, as shown in Fig. 3(b), the NWs remain in the HRS at the negative voltage range, and the SET still occurs once a positive voltage is applied. Therefore, the SET process occurs only at an applied positive voltage, while the RESET process only occurs at negative voltage. The switching behavior is not symmetric.

Fig. 3(d) shows the I-V curve obtained for another fresh Si_2Te_3 NW, which was measured by applying an initial voltage ranging from 0 to a negative value. One can see that the first SET process occurs at -0.6 V followed by a few more current switching events at more negative voltage. As the voltage scans back from -3.0 V to 0 V, the LRS stays unchanged. Then, once a positive voltage is applied, the RESET process occurs at approximately 0.9 V. It takes a few steps for the NWs to complete the RESET process (back to its original resistance). After RESET, the NWs remain in the HRS when the voltage is scanned from 3.0 to 0 V. Experiments were also carried out by starting the voltage scan from zero to +3.0 V first for this sample, interestingly, no current switching using an applied positive voltage was observed, but switching does occur for an applied negative voltage, as shown in Fig. 3(e). This observation shows that the SET from the HRS to LRS occurs only at negative voltage, while the RESET occurs only at positive voltage.

The experimental data shown in Fig. 3 clearly indicate that the SET and RESET conditions for the two samples are different. Each one has its own polarity for the resistance switching. By analyzing a large number of samples, we find that the initial voltage scan for fresh samples determines their SET and RESET to occur at positive or negative voltage. If the first scan starts from 0 to positive voltage, a SET process from the HRS to LRS is programmed to occur at positive voltage. The NWs permanently inherit the SET at positive voltage and RESET at negative voltage sequence. However, if the initial applied voltage ranges from 0 to a negative value for the SET process, then the device shows an SET at negative voltage and a RESET at positive voltage. Therefore, the polarity of the voltage applied to a freshly prepared NW for inducing resistance switching for the first time permanently defines the SET and RESET conditions in the NW. This initial applied voltage for switching is believed to cause a permanent change in the NWs, which is difficult to completely reverse afterwards.

The resistance switching behavior is repeatable for individual NWs as well as a large number of NW samples. Figs. 3(c) and 3(f) show repeated SET and RESET for resistance switching for two types of "programmed" NWs using different polarities for the initial voltage. Each experiment is carried out by scanning the voltage for 10 cycles. Although the voltages at which the SET and RESET occur are slightly different from one cycle to another, the overall switching behavior is well-reproduced each time. The stability of the NWs in the HRS and LRS states was studied by monitoring the current under a constant voltage of 0.1 V over time. The current in both states is extremely stable without a noticeable change observed over 2000 s as shown in Fig. 4.

The resistance switching properties have been studied for other semiconductors. ^{15–20} The switching mechanism generally involves formation of metal filaments, phase change from crystalline to amorphous upon application of the voltage, Schottky barrier²¹ and Poole-Frenkal emission. ²² The resistance switching behavior in the Si₂Te₃ NWs cannot be explained by the crystalline to amorphous phase change as such a mechanism is usually unipolar rather than bipolar as observed in in Si₂Te₃. It is also unlikely due to the formation/rupture of nanoscale metal filaments, as no mobile metal ions are present. The contact effect is also excluded because the switching behavior is independent of electrode materials as being used in this study. The role of surface SiOx if any played in the switching can be also excluded because the field strength along the NW is too low and the current mainly

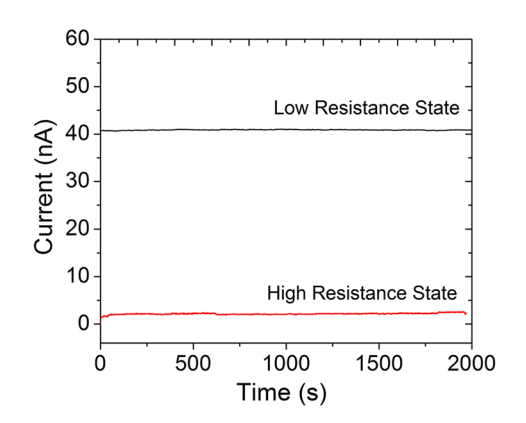


FIG. 4. A stability test for devices in the high and low resistance states with an applied constant voltage of 100 mV.

through Si₂Te₃ NW is not high enough to induce filament formation from SiOx. In addition, the I-V curve becomes linear after switching to LRS, which suggest metallic phase is achieved. Filament and other current mechanisms cannot explain the metallic conducting in Si₂Te₃ NWs.

Based on the results obtained from first-principles calculations, we propose that the resistive switching in Si_2Te_3 NWs originates from a unique phase transition: when an external voltage is applied along the NWs, the Si-Si dimers in Si_2Te_3 dissociate under the effect of Joule heating, with one of the two Si atoms in the dimer migrating across the top of the Te bilayer under the electric field, causing the Si_2Te_3 to restructure into a metastable metallic phase (Fig. 5). We have carried out structural optimization of the model for restructured Si_2Te_3 (Fig. 5(b)) using density functional theory and found that this structure is indeed metastable. We also calculated the electronic density of states for the restructured phase, which shows a metallic feature (Fig. 5(d)) compared to the original semiconducting Si_2Te_3 phase (Fig. 5(c)). Therefore, the restructuring shown in Figs. 5(a) and 5(b) can explain the resistive switching in Si_2Te_3 NWs. This switching mechanism explains the bipolar switching behavior because an opposite voltage is required to move the migrated Si atom back to its original position. This mechanism also explains the multiple resistance states observed for the NWs during switching because restructuring can occur in different segments of the NWs instead of the whole NW, as illustrated in Fig. 5(e).

This mechanism is also further supported by the experimental data obtained for the number of SET and RESET steps. When only one SET occurs (i.e., one resistance switching), only one recovering step is needed and observed. This corresponds to one segment of nanowires being switched. As the number of SET steps increases, i.e., more segments participate in the transition from semiconducting to metallic, the RESET process also requires more RESET steps of the same number to switch the

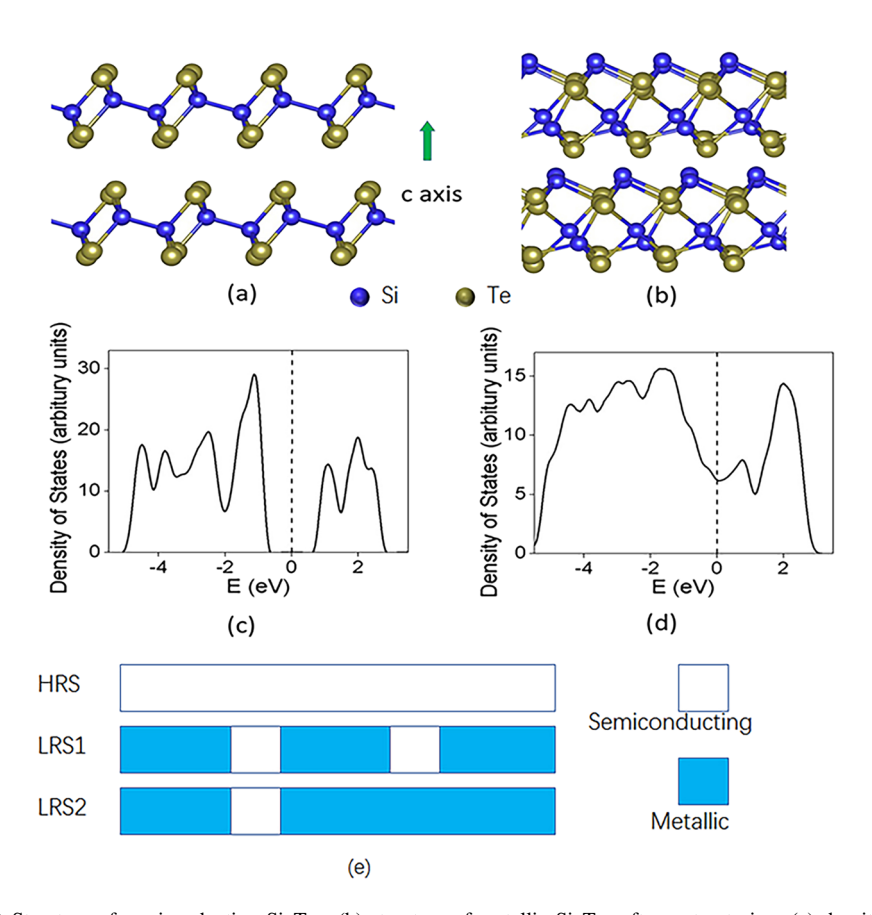


FIG. 5. (a) Structure of semiconducting Si_2Te_3 ; (b) structure of metallic Si_2Te_3 after restructuring; (c) density of states for semiconducting Si_2Te_3 ; (d) density of states for metallic Si_2Te_3 calculated by density functional theory (DFT); and (e) illustration of switching from the high-resistance state (HRS) to multiple low-resistance states (LRSs).

NWs back to their original state. This observation agrees well with the proposed mechanism that involves switching of the different segments of the NWs, as shown in Fig. 5(e).

It should be noted that the as-fabricated NWs show symmetric switching, as the first SET process can occur under either positive or negative voltages. However, after the first SET, the polarity of the NW is fixed. This phenomenon can be understood by the fact that it is likely that after the first SET and RESET, not all atoms of the restructured metallic Si₂Te₃ are switched back to the original position. The metallic phase of the Si₂Te₃ shows a permanent electrical dipole moment due to the asymmetric distribution of Si and Te along the c-axis (Fig. 5(b)), and the parts of the NW that have not switched back to the semiconducting phase will show an electrical dipole moment in the same direction as the first SET voltage. If one attempted to SET the NWs using the opposite voltage, the remaining electrical dipole moments will cancel the external electric field and prevent the SET process.

In conclusion, single-crystalline Si₂Te₃ nanowires are grown by CVD with the assistance of a gold catalyst. The Si₂Te₃ nanowires show layer-by-layer growth along the [0001] direction, i.e., layer by layer stacking along the nanowire axis. The resistance of the nanowires can be reversibly switched between high or low resistance states by applying an electric potential, which demonstrates that the Si₂Te₃ nanowires are a promising candidate for resistive memory devices. The polarity of the bipolar switching can be "programmed" by the polarity of the initial voltage applied to a freshly prepared nanowire. The resistance switching behavior is explained by a phase transition between metallic and semiconducting segments along the nanowires, as supported by both experimental data and theoretical calculations.

This work was supported by the National Science Foundation (1709528), and Natural Science foundation of Educational Commission of Anhui Province of China (KJ2015A150). Computational resources were provided by the High-Performance Computing Facility at the University of Memphis, and by the NSF XSEDE under grants TG-DMR 170064 and 170076.

```
<sup>1</sup> S. Steinberg, R. P. Stoffel, and R. Dronskowski, Cryst. Grow. Des. 16, 6152 (2016).
<sup>2</sup>G. Gregoriades, G. L. Bleris, and J. Stoemenos, Acta Cryst. B 39, 421 (1983).
<sup>3</sup> X. Shen, Y. S. Puzyrev, C. Combs, and S. T. Pantelides, Appl. Phys. Lett. 109, 113104 (2016).
<sup>4</sup>S. Keuleyan, M. Wang, F. R. Chung, J. Commons, and K. J. Koski, Nano Lett. 15, 2285 (2015).
<sup>5</sup> K. Wu, W. Sun, Y. Jiang, J. Chen, L. Li, C. Cao, S. Shi, and J. Cui, J. Appl. Phys. 122, 075701 (2017).
<sup>6</sup> K. Wu and J. Cui, Journal of Materials Science: Materials in Electronics 29, 15643 (2018).
<sup>7</sup> M. J. Wang, G. Lahti, D. Williams, and K. J. Koski, ACS Nano 12, 6163 (2018).
<sup>8</sup> P. Hohenberg and W. Kohn, Phys. Rev. 136, B864 (1964).
<sup>9</sup> W. Kohn and L. Sham, J. Phys. Rev. 140, A1133 (1965).
<sup>10</sup> J. Perdew, K. Burke, and M. Ernzerhof, Phys. Rev. Lett. 77, 3865 (1996).
<sup>11</sup> G. Kresse and D. Joubert, Phys. Rev. B 59, 1758 (1999).
<sup>12</sup> G. Kresse and J. Furthmuller, J. Phys. Rev. B 54, 11169 (1996).
<sup>13</sup> H. Monkhorst and J. D. Pack, J. Phys. Rev. B 13, 5188 (1976).
<sup>14</sup> K. Ziegler and U. Birkholz, Phys. Status Solidi A 39, 467 (1977).
<sup>15</sup> D. Panda and T. Y. Tseng, Ferroelectrics 471, 23 (2014).
<sup>16</sup> H. D. Kim, H. M. An, K. C. Kim, Y. Seo, K. H. Nam, H. B. Chung, E. B. Lee, and T. G. Kim, Semicond. Sci. Technol. 25,
```

¹⁷ P. Nukala, C. C. Lin, R. Composto, and R. Agarwal, Nat Commun. 7, 10482 (2016).

¹⁸ J. S. Lee, S. Brittman, D. Yu, and H. K. Park, J. Am. Chem. Soc. **130**, 6252 (2008).

¹⁹ S. W. Nam, H. S. Chung, Y. C. Lo, L. Qi, J. Li, Y. Lu, C. Johnson, Y. Jung, P. Nukala, and R. Agarwal, Science 336, 1561 (2012).

²⁰ A. Sharma, B. Bhattacharyya, A. K. Srivastava, T. D. Senguttuvan, and S. Husale, Scientific Reports 6, 19138 (2016).

²¹ C. Funck, A. Marchewka, C. Bäumer, P. C. Schmidt, P. Müller, R. Dittmann, M. Martin, R. Waser, and S. Menzel, Adv. Electron Mater. 4, 1800062 (2018).

²² A. Sawa, Materials Today 11, 28 (2008).